GeoPlanning

Journal of Geomatics and Planning

Geoplanning: Journal of Geomatics and Planning, Vol. 13, No. 1, 2026, 21 - 34

e-ISSN: 2355-6544

Received: 18 June 2025;
Revised: 26 May 2026;
Accepted: 30 May 2026;
Available Online: 15 June 2026;
Published: 15 June 2026.

Keywords:
Landslide Investigation, Satellite Remote Sensing, Numerical Modeling, Slope Failure, Kennon Road

*Corresponding author(s)
email: raramirez@ust.edu.ph

Original Research Open access

Landslide Investigation Based on Satellite Remote Sensing and Numerical Modeling: A Case Study of Slope Failure in Kennon Road, Benguet, Philippines

Ryan Angeles Ramirez[1,2,3]*, Jann Rheynald Cañeda[2], Irvin Olchondra[2], Mark Morales[2]

1. *Department of Civil Engineering, University of Santo Tomas, Manila 1015, Philippines*
2. *PGA Earth Structures Solution, Inc., Quezon 1103, Philippines*
3. *Division of Earth and Space Sciences, National Research Council of the Philippines, Taguig 1631, Philippines*

DOI: 10.14710/geoplanning.13.1.21-34

Abstract

The structural stability and serviceability of transport infrastructure in mountainous regions are increasingly compromised by climate- and human-induced geohazards. Traditional ground-based geodetic monitoring methods, while reliable, are often limited by high costs, labor demands, and restricted spatial coverage. This study aims to develop a cost-effective monitoring framework integrating satellite remote sensing and numerical stability analysis to detect precursory slope movements in mountainous terrains. The study utilized 43 Sentinel-1 (S1) C-band SAR images acquired between January 10, 2022, and May 29, 2023. Using the Persistent Scatterer Interferometric SAR (PSInSAR) method, the research monitored a critical section of Kennon Road in Benguet, Philippines. The S1-PSInSAR analysis identified precursory instability beginning in March 2023, approximately two months before a major slope failure occurred on May 31, 2023, due to heavy rainfall from a super typhoon. The results indicate a maximum cumulative displacement of 34 mm along the radar line-of-sight. These findings were cross-validated using limit equilibrium analysis in Slide2 software, which yielded safety factors (FS) significantly below unity for all methods, confirming the inherent instability of the slope even under dry conditions. The study concludes that despite technical challenges such as dense vegetation and atmospheric interference in mountainous terrain, the integrated PSInSAR and numerical modeling approach provides a viable, near-real-time tool for enhancing the resilience of transport infrastructure networks in the Philippines.

Copyright © 2026 by Authors,
Published by Universitas Diponegoro Publishing Group.
This open-access article is distributed under a
Creative Commons Attribution 4.0 International license

1. Introduction

Monitoring transport infrastructure conditions, such as highways, bridges, railways, and airports, is critical for asset owners and administrators to guarantee structural stability, operational safety, and usability and to prevent damage and deterioration, leading to expensive rehabilitation or worse failures and collapses (Chang et al., 2003). Several non-destructive testing (NDT) methods are available for ground surface displacement detection, mapping, and monitoring, including Global Navigation Satellite System (GNSS), precise leveling, Ground Penetrating Radar (GPR), Infrared Thermography (IRT), and Terrestrial Laser Scanning (TLS) (Albattah, 2003; Lagüela et al., 2018; Saarenketo & Scullion, 2000; Sato et al., 2003; Sevil et al., 2020). However, these NDT methods are time-consuming, costly, require many workforces, and are challenging to implement at a regional scale due to economic and administrative constraints.

In recent decades, several free-of-use space-borne data from Synthetic Aperture Radar (SAR) have been exploited in many regions around the globe for ground surface displacement detection, mapping, and monitoring. Innovative, advanced, and multi-temporal SAR-based techniques, including the Persistent Scatterer Interferometric SAR (PSInSAR) (Ferretti et al., 2001), have been developed, evolved, and gained interest in transport infrastructure monitoring and investigating nearby areas (Bianchini Ciampoli et al., 2020; Chang et al., 2017; D'Amico et al., 2020; Gao et al., 2016; Guzman-Acevedo et al., 2023; Kizilirmak & Cakir, 2024; Ramirez et al., 2022).

The unprecedented availability of free Sentinel-1 (S1) SAR data has introduced the Philippines to InSAR technology. Recent studies reported applications of SAR data and InSAR techniques for earth observation purposes in the Philippines. These applications include the detection and mapping of ground surface deformations and damages induced by earthquakes (Abcede et al., 2022; Li et al., 2020; Tiongson & Ramirez, 2022), volcano eruptions (Bato et al., 2021; Ramirez & Abdullah, 2022), and landslides (Mayuga et al., 2022). SAR data has also been applied for drought risk assessment and monitoring at a regional scale (Alonzo et al., 2023). Specifically, the PS-InSAR technique has been successfully used for monitoring urban subsidence (Espiritu et al., 2022; Ramirez et al., 2022; Reyes et al., 2022) and landslides (Ramirez et al., 2023). However, despite these recently reported SAR-related studies in the Philippines, the complexity of InSAR processing hinders understanding of landslide mechanisms and the near-real-time monitoring of unstable slopes, specifically those adjacent to transport infrastructures in highly mountainous regions. Additionally, InSAR-related landslide studies are seldom cross-validated and (or) integrated with other conventional geotechnical solutions, including numerical modeling (Necula et al., 2021; Sun et al., 2023; Tian et al., 2022; Wang et al., 2024; Zhang et al., 2024).

This study addresses this gap by integrating PSInSAR with limit equilibrium numerical modeling (Slide2). The novelty lies in integrating geotechnical numerical modeling with satellite-derived deformation data to validate site-specific instabilities. This approach offers a scalable, non-destructive framework for enhancing highway resilience. Given the lack of near-real-time, cost-effective, and non-destructive ground surface displacement monitoring systems in the Philippines, this study presents how satellite remote sensing data and techniques can detect and monitor transport infrastructure assets in highly mountainous regions.

Specifically, this research aims to evaluate the capability of S1-PSInSAR to detect precursory slope instability in high-relief mountainous terrain and cross-validate satellite findings with numerical FS calculations. The case study presented in this paper focuses on applying the PSInSAR technique based on the S1 SAR data to detect and monitor precursory slope movement along Kennon Road in Benguet Province, Philippines. The case study focused on a localized slope failure adjacent to an ongoing retaining wall construction in Camp 6 in Tuba town that occurred on May 31, 2023, due to a super typhoon.

This research demonstrates the application of a cost-efficient NDT tool, leveraging free-to-use SAR data and an open-source PSInSAR software package, for regional transport infrastructure asset monitoring in mountainous regions of the Philippines, complementing numerical simulation tools for various geotechnical applications. These tools are critical to appraise transport infrastructure assets appropriately, specifically during and after the onset of geological- and hydro-meteorological-driven hazards in the Philippines. Accordingly, this research supports the Philippine Space Agency's (PhilSA) activities related to space science and technology applications and utilizations, specifically enhancing hazard management and disaster mitigation strategy and ensuring the nation's resiliency to climate change.

2. Data and Methods

2.1. Study Area

The region of interest (ROI) is Benguet Province in the Philippines, as shown in Figure 1. Specifically, the site investigated and monitored is National Route 54 (N54) Kennon Road, a highway built on mountains. Kennon Road is a two-lane mountain road with an approximately 34 km stretch that connects Baguio City and Benguet to the lowland town of Rosario and La Union Province (Napaldet, 2023). Most of the stretch of Kennon Road

encompasses the municipality of Tuba in Benguet Province. Moreover, the road was cut above and follows the Bued River course.The ROI falls under a tropical savanna climate based on the Köppen climate classification. The climate is generally tropical, with most months of the year marked by significant rainfall and a short dry season. The mean yearly temperature is 21.4°C, and precipitation is 269.1 cm. The ROI is highly susceptible to rainfall-induced landslides, with a history of numerous old landslide records. The site is approximately 6.5 km west of the Tebbo Fault, making the site susceptible to earthquakes and earthquake-induced landslides. Additionally, the site is approximately 136.9 km north of the nearest volcano, Mt. Pinatubo, and only 5.1 km northwest of the inactive Santo Tomas Volcano. Despite the short distance, no immediate volcanic hazard threat has been reported.

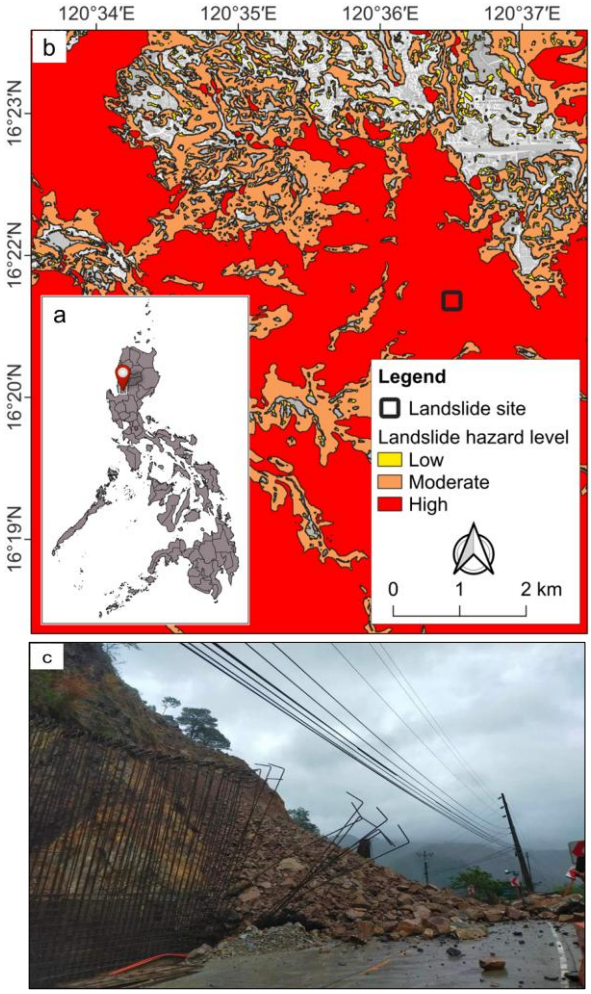

Source: Analysis, 2025

Figure 1. (a) Location of the Region of Interest (ROI) in the Philippines, (b) Landslide Hazard Map Over Benguet, Philippines, and (c) Localized Slope Failure at Kennon Road, Camp 6, Tuba, Benguet

On May 31, 2023, at around 9:00 am, a section of Kennon Road along Camp 6 in Tuba town (16°21'13.558" N, 120°36'35.104" E) collapsed, as shown in Figure 1c, due to a failed road slope. This slope failure occurred during Super Typhoon Betty (local name), which hit the northern part of the Philippines. This slope failure damaged the adjacent retaining wall currently being constructed, blocking the roadway and compromising traffic in the ROI. The local government reported no casualties. The retaining wall construction is one of the mitigation measures implemented along Kennon Road to protect vehicles and motorists traversing the area. The construction started in January 2023.

2.2. Sentinel-1 SAR Dataset

This The twin S1 satellites provide medium-resolution SAR data in all-weather and day-and-night conditions. These SAR data are freely distributed for scientific and research purposes under the Copernicus joint initiative of the European Space Agency (ESA) and the European Commission (EC). S1 satellites are equipped with a C-band having a wavelength of 5.6 cm. This study exploited 43 S1 SAR data acquired by the descending S1 satellite from January 10, 2022, to May 29, 2023. The SAR data acquired by the descending S1 satellite was used since the specific slope section along Kennon Road under investigation faces southwest.

The retaining wall construction along Kennon Road significantly alters the ground surface topology, leading to the inability of the PSInSAR technique to detect slope movement. Hence, a shorter S1 SAR data coverage (i.e., 1 year and 4 months) is considered, allowing better detection of ground instability before the slope failure on May 31, 2023, in Kennon Road in Camp 6, Tuba town. The S1 SAR image acquired on August 26, 2022, was set as the master image, as shown in Figure 2, to mitigate the effect of spatiotemporal decorrelation. The master image is selected under the following criteria – acquired under satisfactory weather conditions (i.e., little to no precipitation) and produces the optimal perpendicular and temporal baseline with the slave images (Espiritu et al., 2022). The weather condition for the software-selected master image was confirmed using weather data from the Philippine Atmospheric, Geophysical and Astronomical Services Administration (PAGASA).

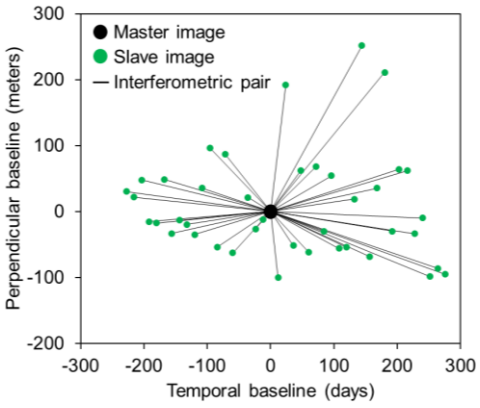

Source: Analysis, 2025

Figure 2. Sentinel-1 Synthetic Aperture Radar (S1 SAR) Dataset and Interferometric Pairs

2.3. PSInSAR Analysis

Flood Two main processing stages were implemented for S1-PSInSAR analysis, as shown in Figure 3: Sentinel Application Platform (SNAP) pre-processing and Stanford Method for Persistent Scatterers (StaMPS) processing. The SNAP-StaMPS workflow was adopted following the approach of Shi et al. (2021), who utilized similar methods to mitigate atmospheric phase delay in mountainous terrains. The first stage was accomplished using SNAP for the master image selection (i.e., using the InSAR Stack Overview) and the snap2stamps package tool for the single master-slave images co-registration, interferogram formation, and topographic phase removal utilizing the Shuttle Radar Topography Mission Digital Elevation Model (SRTM DEM) 1 arcsec data in the SNAP Library (Foumelis et al., 2018).

The second stage was accomplished using StaMPS software for the time series InSAR analysis (Hooper et al., 2012). An amplitude dispersion index (ADI) of 0.40, a standard recently validated by Wang et al. (2024), was used to recognize introductory PS candidates (PSCs), launching the StaMPS processing through Matlab. Afterward, the PSCs' phase noise level was estimated iteratively. Based on the noise level, PSs were selected, and the strident ones were dropped. The remaining PSs in the wrapped phase were then amended for spatially uncorrelated look angle error. Afterward, the Statistical-cost, Network-flow Algorithm for Phase Unwrapping

(SNAPHU) was used for phase unwrapping (Chen & Zebker, 2001). Then, the spatially correlated look angle error (i.e., the error in the DEM itself and the imprecise aligning of the DEM into radar coordinates) was approximated and removed from the unwrapped dataset. Lastly, atmospheric effects were mitigated using spatiotemporal filters. Only PSs with temporal coherence >0.7, signifying high-coherent surfaces, were kept for further analysis.

Source: Analysis, 2025

Figure 3. Dual-track Methodology for Landslide Investigation

The immediate results after Stage 2, such as the line-of-sight (LOS) mean displacement velocity map and time series, are relative measures concerning a selected reference area. For this purpose, a preliminary S1 PSInSAR analysis with an ADI of 0.60 was performed, introducing more PSCs corrupted with noise (Ramirez, et al., 2022). Then, the ROI was inspected for a stable reference area by evaluating the LOS mean displacement velocity and time series of PS groups within a moving window with a 50-m radius in StaMPS-Visualizer (Höser, 2018). The mean velocity within the selected reference area must be between ±1 mm/yr with a nearly horizontal LOS displacement time series. The temporal coherence of the selected reference area was close to unity. Finally, the LOS mean displacement velocity map was exported for post-analysis and visualization in the Quantum Geographic Information System (QGIS).

2.4. Slope Stability Analysis Using Numerical Modeling

The limit equilibrium methods, including Bishop's simplified, Ordinary/Fellenius, Janbu Simplified, and Spencer's three-part wedge method, implemented in the commercially available Slide2 numerical simulation software (Rocscience, 2020), were adopted in this study to assess the stability of the investigated slope in the ROI. The Slide2 software can automatically search all predefined potential failure surfaces of the slope and obtain the most critical failure surface with the minimum safety factor (FS). The slope stability analysis was conducted under static and dynamic (earthquake) loading conditions.

The surface model geometry was estimated and constructed using Google Earth Street images. Input values to geotechnical properties used for the numerical model were taken from available literature (Necula et al., 2021; Sun et al., 2023; Tian et al., 2022) due to the lack of actual field and laboratory measurements. These geotechnical properties include the unit weight, soil cohesion, and internal friction angle, as summarized in Table 1. The groundwater table was assumed to be a few meters below the ground surface. The horizontal peak ground acceleration coefficient was considered 0.40 for the dynamic loading condition.

Table 1. Simulation Parameters of the Cut Slope in Kennon Road, Benguet, in the Philippines

Soil Layer	Unit Weight, γ (kN/m^3)	Soil Friction Angle, ϕ (°)	Cohesion, c (kPa)
1	18	30	0
2	20	40	0
3	22	40	0

3. Results and Discussion

3.1. Pre-Failure Mean Annual Velocity Map

The Figure 4 displays the ROI's pre-failure LOS mean annual displacement velocity map retrieved from the S1 SAR dataset. A total of 39,062 PSs were detected in the ROI. Warm colors represent a movement away from the radar, and cold colors indicate movement towards the radar. Most PSs move away from the radar when the S1 satellite descends north to south. Approximately 90.5% of the total PSs have a LOS mean displacement velocity between ±5 mm/yr, as shown in Figure 5.

Most of the PSs were recognized over built-up areas in the mountainous region of Benguet. Additionally, PSs were also detected over roads. However, over forested areas, there is either a partial or complete absence of PSs, as these areas are subject to rapid surface changes between consecutive S1 SAR images. Interestingly, the section along Kennon Road in Camp 6, Tuba town, shown in Figure 4, where an actual failure occurred on May 31, 2023, provided several recognized PSs. These PSs, presumably, represent exposed rocks on the cut slope section of the road. However, the LOS mean displacement velocity of these recognized PSs ranges between ±5 mm/yr, which is lower than those found in the literature, producing massive slope failures (Necula et al., 2021; Ramirez et al., 2023; Sun et al., 2023; Tian et al., 2022).

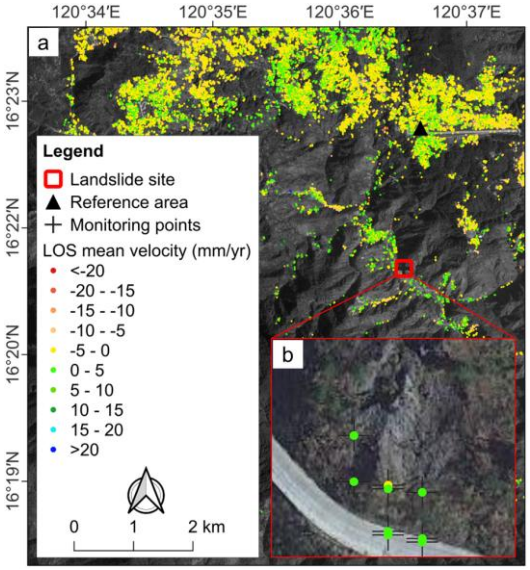

Source: Analysis, 2025

Figure 4. (a) Line-of-Sight (LOS) Mean Displacement Velocity Map over the ROI in Benguet, Philippines, and (b) Recognized Persistent Scatterers (PSs) over the Failed Slope along Kennon Road

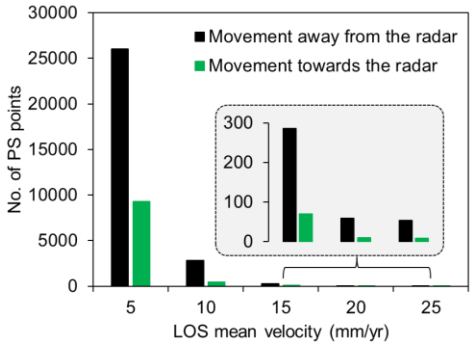

Source: Analysis, 2025

Figure 5. LOS Mean Displacement Velocity Distribution for PSs over the ROI. The Inset Shows the Number of PSs with LOS Mean Displacement Velocity Outside the ±15 mm/yr Range

3.2. Pre-failure LOS Displacement Time Series

The PSInSAR analysis identified a distinct acceleration in displacement starting in March 2023, as shown in Figure 6a. This figure shows the mean cumulative LOS displacement time series of nine representative PS over the landslide zone. The daily and accumulated rainfall values are also plotted in Figure 6b. The rainfall data were acquired from the nearest rain gauge station operated by PAGASA. The precipitation from the rainfall events from January 2022 to December 2022 may have led to waterlogging on the ground (Ramirez et al., 2023). The waterlogged effect is evident in the mean cumulative LOS displacement time series (i.e., highlighted with light blue). This effect suggests that the slope's internal drainage was likely compromised by previous saturation cycles in 2022. This led to a reduction in effective stress within the soil mass, which PSInSAR captured as a steady "creeping" phase. This interpretation strengthens the findings by showing that the satellite was not just recording a landslide in progress, but rather the pre-failure strain of the slope as it reached a critical state. However, from January 2023 to March 2023, the slope section stabilized before it showed a more pronounced instability before the actual failure on May 31, 2023. The daily rainfall was more than 170 mm one day before the slope failed.

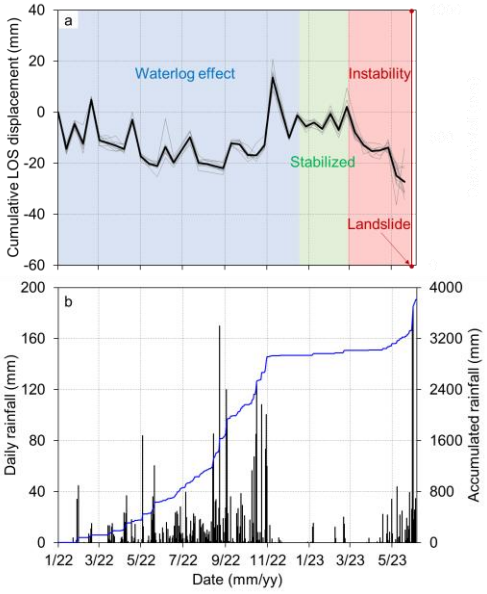

Source: Analysis, 2025

Figure 6. (a) Mean Cumulative LOS Displacement Time Series of Nine Representative PSs in the Landslide Site and (b) Rainfall Data

On the one hand, the daily rainfall recorded on the day the slope failed was more than 180 mm. Additionally, the accumulated rainfall from May 1, 2023, to May 30, 2023, has reached 400 mm. The global precipitation threshold triggering landslides is about 100 mm/day (Catane et al., 2019). At the end of the slope monitoring period, two days before the slope section collapsed, the minimum, maximum, and mean cumulative LOS displacements were −14 mm, −34 mm, and −27 mm, respectively. The identified maximum cumulative displacement of 34 mm aligns with findings by Han et al. (2023) and Zhang et al. (2024b), who noted that displacement exceeding 30 mm often serve as a critical threshold for imminent failure. Furthermore, the detection of precursory movement two months prior to the May 31 failure demonstrates a monitoring lead time consistent with the "acceleration phase" reported in similar highway slope failures in Southern Chine (Zhang et al., 2024).

3.3. Preliminary Slope Stability Assessment

The limit equilibrium method implemented in the Slide2 numerical software package was used to investigate the effect of the cut slope at the landslide site on the overall FS using different limit equilibrium methods. The slope is stable when the minimum FS calculated for the critical failure surface is 1.5 and 1.1 for the static and dynamic loading conditions, respectively, for all methods.

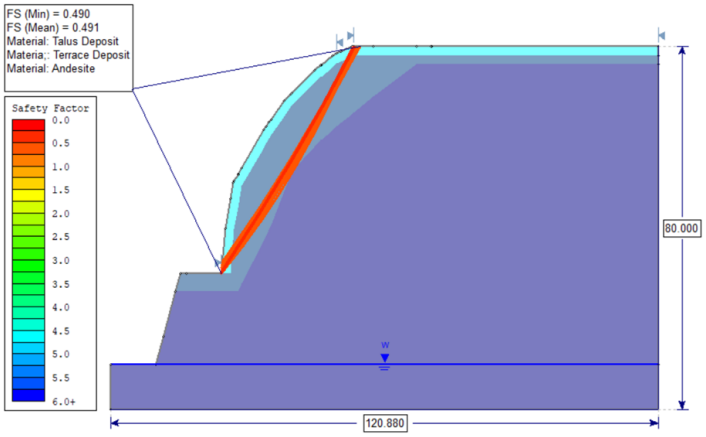

Source: Analysis, 2025

Figure 7. Limit Equilibrium Analysis of the Cut Slope Considering Static Loading Conditions

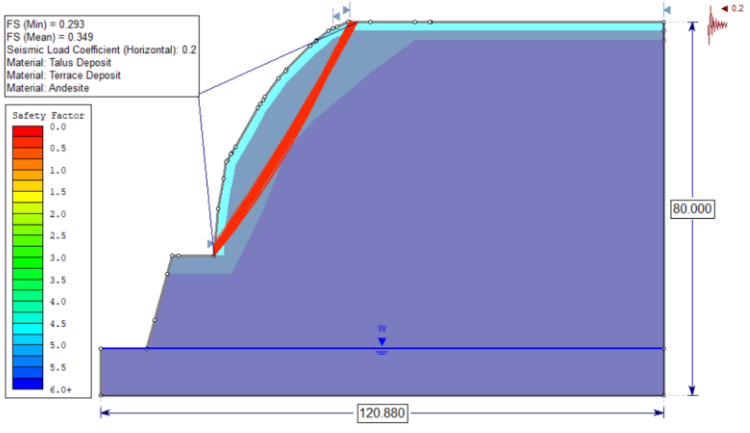

Source: Analysis, 2025

Figure 8. Limit Equilibrium Analysis of the Cut Slope Considering Dynamic Loading Conditions

Analyses of the modeled cut slope section under the static and dynamic loading conditions with unsaturated strength parameters yielded FS below unity for all methods, as shown in Figure 7, Figure 8, and Table 2. These numerical findings imply that the cut slope may be unstable even under dry conditions. Unsatisfactory FS, nevertheless, supports the observed instability of the cut slope since March of 2023, as shown in Figure 6a, despite a relatively low LOS mean displacement velocity from the S1-PSInSAR analysis. The fact that the FS was below unity even under dry conditions explains why the PSInSAR was able to detect constant, millimeter-scale movement months before the ultimate collapse. In elevated pore water pressures due to slope saturation (i.e., rainfall infiltrating the fissures on the rocky slope) during downpours and (or) dynamic loading, further instability of the cut slope is expected. Exposing the potential shallow failure surfaces due to surficial soil support may have contributed to the increase in shear stress and decrease in the available shear strength of the slope material (Catane et al., 2019).

Recent research by Lu et al. (2024) emphasizes that rainfall is the primary trigger for landslides in Southeast Asia; however, the study's results indicate that the Kennon Road slope was already at a critical state (FS<1.0) even under dry conditions. This condition corroborates the pre-conditioning factors identified by Mandal & Saha (2025), where long-term creeping movements detected by SAR are indicative of structural soil fatigue before the final rainfall-triggered collapse. The cross-validation with Slide2 proves that the rainfall from the super typhoon was merely the final trigger for a slope that was already geotechnically failed or at a state of meta-stability. This connection demonstrates the robustness of the monitoring framework. The PSInSAR identifies the "where and when" of the movement, while the numerical modeling explains the "why" by quantifying the insufficient shear strength of the soil profile.

Table 2. Minimum Safety Factors for the Modeled Cut Slope

Soil Layer	Minimum Safety Factor	
	Static Loading Case	Dynamic Loading Case
Ordinary/Fellenius	0.50	0.30
Bishop simplified	0.50	0.30
Janbu simplified	0.50	0.30
Spencer	0.50	0.50
GLE/Morgenstern-Price	0.50	0.40

3.4. Limitations, Future Works, and Practical Implications

The results move beyond description by highlighting the predictive capability of the integrated approach. The correlation between the accelerating displacement curve in Figure 6a and the low FS in Table 2 suggests that a critical displacement threshold can be established for Kennon Road. For transport authorities, this means that once PSInSAR detects cumulative movement exceeding a specific limit, immediate geotechnical intervention or traffic diversion should be mandated, regardless of whether a visible failure has occurred. This transforms the results from post-mortem case study into a proactive hazard mitigation tool.

However, the successful application of the S1-PSInSAR technique for landslide investigation is influenced by several factors. Constantly changing ground surface topology makes detecting high-density and high-quality PS points challenging (Tian et al., 2022). These surface changes can be attributed to human-induced activities, including cutting slopes for road widening purposes and constructing slope protection systems, including safety nets and retaining wall construction, which are primarily implemented along Kennon Road. The constant movement of slope vegetation cover due to blowing wind amplifies abrupt surface changes, leading to a complete loss of the SAR signal. Additionally, the mountainous terrain nature of the ROI contributes to the atmospheric effect, hindering effective mitigation using the S1-PSInSAR technique or other advanced multi-temporal InSAR implementations (Shi et al., 2021; Wang et al., 2024). This effect causes over- or underestimation of the ground surface deformation, resulting in inconsistent and inaccurate slope precursory movement detection and monitoring. Geometric distortions (i.e., foreshortening, layover, enhanced resolution, and shadow) due to the

right-side-looking nature of the S1 satellite may also miscalculate precursory slope movement in mountainous regions (Shi et al., 2024). Nevertheless, adapting second-generation advanced InSAR techniques, including SqueeSAR (Ferretti et al., 2011), can significantly improve ground target detection. SqueeSAR jointly processes PS and distributed scatterers, thus increasing ground target recognition, especially in highly mountainous regions like Benguet Province. Moreover, a multi-temporal moving-window linear model can be incorporated in the S1-PSInSAR analysis stage as a substitute for spatiotemporal filtering to correct the atmospheric delay for wide-area landslide investigation (Wang et al., 2022). A layover and shadow map ground-range slope method can also improve the discrimination of subtle geometric distortions within complex mountainous terrains (Shi et al., 2024).

The numerical modeling phase, coupling the S1-PSInSAR detection of an unstable slope, also presents challenges that could lead to erroneous FS calculation. The study did not account for the influence of elevated pore water pressure on the occurrence of rock falls and landslides (Sun et al., 2023). Elevated pore water pressure due to infiltrating rainfall reduces the slope's shear strength. The numerical model also assumed the rock slope was intact and bore with no cracks (Catane et al., 2019). Such an assumption did not account for crack initiation, propagation, or behavior within the rock slope. Rock slopes often have pre-existing cracks, and the presence and behavior of these cracks can significantly influence the slope's stability and behavior under stress. Due to a lack of in-situ and laboratory test data, the geometric and geotechnical properties assigned to the numerical model were also conservatively assumed. The modeled cut slope most likely has lithological and implicit geotechnical variations, both vertically and horizontally (Necula et al., 2021). Future research could utilize a sophisticated finite difference method (FDM) or finite element method (FEM) to simulate slope stability under rainfall infiltration accurately (Pan et al., 2020). Likewise, this FDM or FEM can be extended to account for the numerical simulation of the non-intact rock failure process (Li et al., 2024). However, using these advanced and sophisticated tools, in most cases, comes with a cost. Despite these numerical model simplifications, the preliminary slope stability analysis results could explain the abrupt slope failure on May 31, 2023.

Nonetheless, the S1-PSInSAR results presented in this study show the viability of satellite remote sensing technology to provide near-real-time landslide early detection tools over transport infrastructure networks traversing mountain slopes. Once unstable mountain slopes have been detected, the thematic databases, including morphological, geotechnical, hydrological, and meteorological, can be collected and used for numerical and (or) predictive modeling for different potential slope conditions. Numerical simulations further estimate and support the detected slope instability based on the calculated FS. For example, the numerical modeling results confirmed the instability that the S1-PSInSAR technique detected for the investigated cut slopes.

Kennon Road in Benguet Province in the Philippines has been acknowledged as a critical transport infrastructure network susceptible to landslides. Specifically, the investigated landslide site is one of the areas where mountainside mitigation measures are being constructed to protect motorists and pedestrians from possible rockfall or debris from the mountain slope. The Department of Public Works and Highways-Cordillera (DPWH-Cordillera) started constructing reinforced concrete retaining walls, with a length of 151 meters, in January 2023 and targeted to be completed by January 2024. Rockfall incidents were reported in two different slope sections on May 8 and 9, 2023. These rockfalls collapsed the exposed, unbounded steel reinforcements on these slope sections. However, the specific locations of these slope failures are unknown.

Assessing the displacement time series curve obtained from the S1-PSInSAR results can aid in selecting the most efficient, fastest, yet robust slope protection systems that can be constructed to create landslide-resilient transport infrastructures in mountainous regions. The selection of slope protection systems may be based on capturing and reasonably interpreting the ground surface displacement anomaly trends after slope instability confirmation with numerical simulation results. Site inspection of the suspected unstable slopes can also be performed to corroborate both desk analyses.

Lastly, the application of satellite remote sensing technology in this study, paired with numerical modeling, shows its viability as a near-real-time landslide early warning system. This system may facilitate seamless traffic communication and coordination at the onset of heavy downpours in mountainous regions for concerned transport infrastructure authorities, users, and surrounding communities. Transport authorities may control the number of motorists and pedestrians and signal when they can pass through these roads. Likewise, transport authorities can provide alternative, safer routes for motorists and pedestrians. Residents living near suspected unstable slopes can also be evacuated with sufficient lead time and be temporarily housed in a much safer area.

4. Conclusion

This study demonstrates the efficacy of integrating satellite-based PSInSAR with numerical limit equilibrium analysis to monitor and evaluate sloe stability along critical transport corridors. By analyzing 43 S1 images, the research successfully detected precursory deformation at a major landslide site on Kennon Road, Benguet, two months prior to its ultimate failure on May 31, 2023. This finding highlights the potential of S1-PSInSAR as a near-real-time early warning tool, particularly in regions where traditional ground-based monitoring is logistically or financially prohibitive. The primary contribution of this work lies in the cross-validation of satellite-derived displacement data with geotechnical numerical modeling (Slide2), which confirmed that the slope was inherently unstable (FS<1.0) even before the triggering rainfall event. This integrated approach bridges the gap between regional-scale remote sensing and site-specific engineering analysis, providing a more robust framework for infrastructure resilience in the Philippines.

To enhance the technical rigor and continuity of the study, future research should transition toward second-generation InSAR techniques, such as SqueeSAR or Quasi-PS (QPS), to optimize measurement point density across the heavily vegetated terrains of the Philippine cordilleras. To mitigate the geometric and atmospheric distortions inherent to these steep, mountainous areas, upcoming studies must incorporate high-resolution DEMs alongside advanced atmospheric delay models. Furthermore, coupling these refined SAR datasets with hydrogeological modeling, specifically employing FEM or FDM frameworks, will allow researchers to precisely simulate the transient effects of rainfall infiltration and fluctuating pore-water pressure on sloe stability. Finally, integrating and validating these satellite-derived trends with in-situ ground sensors, such as GNSS and inclinometers, is critical to calibrating displacement data and establishing highly reliable empirical early warning thresholds.

5. Acknowledgments

The authors thank the University of Santo Tomas through the Faculty of Engineering and the PGATech Group of Companies through Earth Structure Solutions, Inc., for the assistance and support in conducting and completing this research work.

6. References

Abcede, E. L., Ajesta, A., Alfonso, J. D., Nucup, R. J., Peralta, M., & Ramirez, R. (2022). InSAR-based Detection and Mapping of Seismically Induced Ground Surface Displacement and Damage in Pampanga, Philippines. *ASEAN Engineering Journal*, *12*(2), 1–10. [Crossref]

Albattah, M. (2003). Landslide Monitoring Using Precise Levelling Observations. *Survey Review*, *37*(288), 127–136. [Crossref]

Alonzo, C. A., Galabay, J. M., Macatangay, M. N., Magpayo, M. B., & Ramirez, R. (2023). Drought Risk Assessment and Monitoring of Ilocos Norte Province in the Philippines Using Satellite Remote Sensing and Meteorological Data. *AgriEngineering*, *5*(2), 720–739. [Crossref]

Bato, M. G., Lundgren, P., Pinel, V., Solidum, R., Daag, A., & Cahulogan, M. (2021). The 2020 Eruption and Large Lateral Dike Emplacement at Taal Volcano, Philippines: Insights From Satellite Radar Data. *Geophysical Research Letters*, *48*(7). [Crossref]

Bianchini Ciampoli, L., Gagliardi, V., Clementini, C., Latini, D., Del Frate, F., & Benedetto, A. (2020). Transport Infrastructure Monitoring by InSAR and GPR Data Fusion. *Surveys in Geophysics*, *41*(3), 371–394. [Crossref]

Catane, S. G., Veracruz, N. A. S., Flora, J. R. R., Go, C. M. M., Enrera, R. E., & Santos, E. R. U. (2019). Mechanism of a Low-Angle Translational Block Slide: Evidence from the September 2018 Naga Landslide, Philippines. *Landslides*, *16*(9), 1709–1719. [Crossref]

Chang, L., Dollevoet, R. P. B. J., & Hanssen, R. F. (2017). Nationwide Railway Monitoring Using Satellite SAR Interferometry. *IEEE Journal of Selected Topics in Applied Earth Observations and Remote Sensing*, *10*(2), 596–604. [Crossref]

Chang, P. C., Flatau, A., & Liu, S. C. (2003). Review Paper: Health Monitoring of Civil Infrastructure. *Structural Health Monitoring*, *2*(3), 257–267. [Crossref]

Chen, C. W., & Zebker, H. A. (2001). Two-Dimensional Phase Unwrapping with Use of Statistical Models for Cost Functions in Nonlinear Optimization. *Journal of the Optical Society of America A*, *18*(2), 338. [Crossref]

D'Amico, F., Gagliardi, V., Bianchini Ciampoli, L., & Tosti, F. (2020). Integration of InSAR and GPR Techniques for Monitoring Transition Areas in Railway Bridges. *NDT & E International*, *115*, 102291. [Crossref]

Espiritu, K. W., Reyes, C. J., Benitez, T. M., Tokita, R. C., Galvez, L. J., & Ramirez, R. (2022). Sentinel-1 Interferometric Synthetic Aperture Radar (InSAR) Reveals Continued Ground Deformation in and Around Metro Manila, Philippines, Associated with Groundwater Exploitation. *Natural Hazards*, *114*(3), 3139–3161. [Crossref]

Ferretti, A, Prati, C., & Rocca, F. (2001). Permanent Scatterers in SAR Interferometry. *IEEE Transactions on Geoscience and Remote Sensing*, *39*(1), 8–20. [Crossref]

Ferretti, Alessandro, Fumagalli, A., Novali, F., Prati, C., Rocca, F., & Rucci, A. (2011). A New Algorithm for Processing Interferometric Data-Stacks: SqueeSAR. *IEEE Transactions on Geoscience and Remote Sensing*, *49*(9), 3460–3470. [Crossref]

Foumelis, M., Delgado Blasco, J. M., Desnos, Y.-L., Engdahl, M., Fernandez, D., Veci, L., Lu, J., & Wong, C. (2018). Esa Snap - Stamps Integrated Processing for Sentinel-1 Persistent Scatterer Interferometry. *IGARSS 2018 - 2018 IEEE International Geoscience and Remote Sensing Symposium*, 1364–1367. [Crossref]

Gao, M., Gong, H., Chen, B., Zhou, C., Chen, W., Liang, Y., Shi, M., & Si, Y. (2016). InSAR Time-Series Investigation of Long-Term Ground Displacement at Beijing Capital International Airport, China. *Tectonophysics*, *691*, 271–281. [Crossref]

Guzman-Acevedo, G. M., Quintana-Rodriguez, J. A., Gaxiola-Camacho, J. R., Vazquez-Becerra, G. E., Torres-Moreno, V., & Monjardin-Quevedo, J. G. (2023). The Structural Reliability of the Usumacinta Bridge Using InSAR Time Series of Semi-Static Displacements. *Infrastructures*, *8*(12), 173. [Crossref]

Han, H., Shi, B., Zhang, C.-C., Sang, H., Huang, X., & Wei, G. (2023). Application of Ultra-Weak FBG technology in real-time monitoring of landslide shear displacement. *Acta Geotechnica*, *18*(5), 2585–2601. [Crossref]

Hooper, A., Bekaert, D., Spaans, K., & Arıkan, M. (2012). Recent Advances in SAR Interferometry Time Series Analysis for Measuring Crustal Deformation. *Tectonophysics*, *514–517*, 1–13. [Crossref]

Höser, T. (2018). Analysing the Capabilities and Limitations of InSAR using Sentinel-1 Data for Landslide Detection and Monitoring. *PhD Diss.*, *University of Bonn*.

Kizilirmak, G., & Cakir, Z. (2024). Application of PS-InSAR and Diagnostic Train Measurement Techniques for Monitoring Subsidence in High-Speed Railway in Konya, Türkiye. *Infrastructures*, *9*(9), 152. [Crossref]

Lagüela, S., Solla, M., Puente, I., & Prego, F. J. (2018). Joint use of GPR, IRT and TLS techniques for the integral damage detection in paving. *Construction and Building Materials*, *174*, 749–760. [Crossref]

Li, B., Li, Y., Jiang, W., Su, Z., & Shen, W. (2020). Conjugate Ruptures and Seismotectonic Implications of the 2019 Mindanao Earthquake Sequence Inferred from Sentinel-1 InSAR Data. *International Journal of Applied Earth Observation and Geoinformation*, *90*, 102127. [Crossref]

Li, G., Wang, K., Tang, C., & Ye, J. (2024). Non-break Modeling and Numerical Simulation for Non-Intact Rock Failure Process. *International Journal of Rock Mechanics and Mining Sciences*, *176*, 105725. [Crossref]

Lu, W., Xiao, Z., Chen, Y., Sun, J., & Chen, F. (2024). Spatiotemporal Characteristics and Rainfall Thresholds of Geological Landslide Disasters in ASEAN Countries. *Atmosphere*, *15*(5), 599. [Crossref]

Mandal, S., & Saha, A. K. (2025). A Novel Deep Learning based Spatial Ensemble Approach and Segment Anything Model for Landslide Risk Assessment in Chamoli District of Garhwal Himalayas. *Scientific Reports*, *15*(1), 43592. [Crossref]

Mayuga, P. J., Tiongson, S. F., Abao, J. J., Mendoza, J. M., Pernez, G. A., & Ramirez, R. (2022). Landslide Area Mapping Using Synthetic Aperture Radar (SAR) Data: the Case of The 2018 Naga Landslide. *IGARSS 2022 - 2022 IEEE International Geoscience and Remote Sensing Symposium*, 7883–7886. [Crossref]

Napaldet, J. T. (2023). Plant Species and Ecosystem Diversity Along National Road in Mountain Sites: The Case of Kennon Road in Cordillera Central Range, Philippines. *Taiwania*, *68*(3), 339–348. [Crossref]

Necula, N., Niculiță, M., Fiaschi, S., Genevois, R., Riccardi, P., & Floris, M. (2021). Assessing Urban Landslide Dynamics through Multi-Temporal InSAR Techniques and Slope Numerical Modeling. *Remote Sensing*, *13*(19), 3862. [Crossref]

Pan, Y., Wu, G., Zhao, Z., & He, L. (2020). Analysis of Rock Slope Stability Under Rainfall Conditions Considering the Water-Induced Weakening of Rock. *Computers and Geotechnics*, *128*, 103806. [Crossref]

Ramirez, R. A., & Abdullah, R. E. E. (2022). Damaged Area Mapping and Ground Displacement Estimation using Sentinel-1 Synthetic Aperture Radar (SAR) Interferometry: January 12, 2020, Taal Volcano Eruption Case Study, Philippines. *Mindanao Journal of Science and Technology*, *20*(2).

Ramirez, R. A., Abdullah, R. E. E., & Rubio, C. J. P. (2022). S1-PSInSAR Monitoring and Hyperbolic Modeling of Nonlinear Ground Subsidence in Naga City, Cebu Island in the Philippines. *Geomate Journal*, *23*(100), 102–109. https://geomatejournal.com/geomate/article/view/3751

Ramirez, R. A., Lee, G.-J., Choi, S.-K., Kwon, T.-H., Kim, Y.-C., Ryu, H.-H., Kim, S., Bae, B., & Hyun, C. (2022). Monitoring of Construction-Induced Urban Ground Deformations using Sentinel-1 PS-InSAR: The Case Study of Tunneling in Dangjin, Korea. *International Journal of Applied Earth Observation and Geoinformation*, *108*, 102721. [Crossref]

Ramirez, R., Abdullah, R. E., Jang, W., Choi, S.-K., & Kwon, T.-H. (2023). Satellite-Based Monitoring of an Open-Pit Mining Site using Sentinel-1 Advanced Radar Interferometry: A Case Study of the December 21, 2020, landslide in Toledo City, Philippines. *E3S Web of Conferences*, *415*, 05020. [Crossref]

Reyes, R., Bauzon, M. D. A., Pasaje, N. A., Alfante, R. M., De Lara, P. M., Ordillano, M., Flores, P. C., Rediang, A., Nota, P. A., Siringan, F., Blanco, A., & Bringas, D. (2022). Quantifying Vertical Land Motion at Tide Gauge Sites Using Permanent Scatterer Interferometric Synthetic Aperture Radar and Global Navigation Satellite System Solutions. *Spatial Information Research*, *30*(2), 309–319. [Crossref]

Rocscience. (2020). *Slide2 Software*. Rocscience Inc. https://www.rocscience.com/software/slide2

Saarenketo, T., & Scullion, T. (2000). Road Evaluation with Ground Penetrating Radar. *Journal of Applied Geophysics*, *43*(2–4), 119–138. [Crossref]

Sato, H. P., Abe, K., & Ootaki, O. (2003). GPS-Measured Land Subsidence in Ojiya City, Niigata Prefecture, Japan. *Engineering Geology*, *67*(3–4), 379–390. [Crossref]

Sevil, J., Gutiérrez, F., Carnicer, C., Carbonel, D., Desir, G., García-Arnay, Á., & Guerrero, J. (2020). Characterizing and Monitoring a High-Risk Sinkhole in an Urban Area Underlain by Salt Through Non-Invasive Methods: Detailed Mapping, High-Precision Leveling and GPR. *Engineering Geology*, *272*, 105641. [Crossref]

Shi, C., Zuo, X., Zhang, J., Zhu, D., Li, Y., & Bu, J. (2024). Accuracy Assessment of Geometric-Distortion Identification Methods for Sentinel-1 Synthetic Aperture Radar Imagery in Highland Mountainous Regions. *Sensors*, *24*(9), 2834. [Crossref]

Shi, M., Peng, J., Chen, X., Zheng, Y., Yang, H., Su, Y., Wang, G., & Wang, W. (2021). An Improved Method for InSAR Atmospheric Phase Correction in Mountainous Areas. *IEEE Journal of Selected Topics in Applied Earth Observations and Remote Sensing*, *14*, 10509–10519. [Crossref]

Sun, D., Deng, W., Yang, T., Li, J., & Zhao, Y. (2023). A Case Study Integrating Numerical Simulation and InSAR Monitoring to Analyze Bedding-Controlled Landslide in Nanfen Open-Pit Mine. *Sustainability*, *15*(14), 11158. [Crossref]

Tian, C., Tian, H., Li, C., & Chen, F. (2022). Stability Evaluation of Massive Landslides Using Ensembled Analysis of Time-Series InSAR and Numerical Simulation along the Yellow River, Northwestern of China. *Geofluids*, *2022*, 1–17. [Crossref]

Tiongson, S. F., & Ramirez, R. (2022). Mapping of Ground Surface Deformations and its Associated Damage using SAR Interferometry: A Case Study of the 2020 Masbate Earthquake. *E3S Web of Conferences*, *347*, 03014. [Crossref]

Wang, Y., Dong, J., Zhang, L., Zhang, L., Deng, S., Zhang, G., Liao, M., & Gong, J. (2022). Refined InSAR Tropospheric Delay Correction for Wide-Area Landslide Identification and Monitoring. *Remote Sensing of Environment*, *275*, 113013. [Crossref]

Wang, Z., Jia, Y., Li, S., Zhang, R., Xu, B., & Sun, X. (2024). Landslide-Hazard-Avoiding Highway Alignment Selection in Mountainous Regions Based on SAR Images and High-Spatial-Resolution Precipitation Datasets: A Case Study in Southwestern China. *Remote Sensing*, *16*(7), 1303. [Crossref]

Zhang, Jing, Li, C., Wang, S., Zhang, G., Chen, D., Zhang, P., & Yuan, R.-M. (2024). Deformation and Stability Analysis of the Ancient Da'ao Landslide Revealed by InSAR and Model Simulation. *Landslides*, *21*(4), 829–844. [Crossref]

Zhang, Junrong, Tang, H., Li, C., Gong, W., Zhou, B., & Zhang, Y. (2024). Deformation Stage Division and Early Warning of Landslides Based on the Statistical Characteristics of Landslide Kinematic Features. *Landslides*, *21*(4), 717–735. [Crossref]